Structural Chemistry (2018) 29:667–679
https://doi.org/10.1007/s11224-017-1063-3

ORIGINAL RESEARCH

Solvent impact on the planarity and aromaticity of free and monohydrated zinc phthalocyanine: a theoretical study

Łukasz Gajda[1] · Teobald Kupka[1] · Małgorzata A. Broda[1]

Received: 27 October 2017 / Accepted: 21 November 2017 / Published online: 1 December 2017

Abstract

A theoretical investigation on the planarity of molecular structure of zinc phthalocyanine (ZnPc) and its aromaticity has been performed using B3LYP and M06-2X density functionals combined with selected Pople-type basis sets. The effect of the applied calculation method on the optimized structure of ZnPc and ZnPc···H_2O, both in the gas phase and in the polar solvent, was analyzed. To quantify the aromaticity of the ZnPc and ZnPc···H_2O complexes, both the geometric and magnetic criteria, i.e., Harmonic Oscillator Model of Aromaticity (HOMA) index and the nucleus-independent chemical shift (NICS) values at the centers or 1 Å above the centers of structural subunits, were calculated. The energies of highest energy occupied molecular orbital (HOMO) and lowest energy unoccupied molecular orbital (LUMO) and energy gaps were also estimated. The results show that the free ZnPC molecule is flat in the gas phase and nonplanar in the polar environments (DMSO and water). ZnPC···H_2O is nonpolar in the gas phase and polar solvent which is in agreement with recent X-ray reports. Both HOMA and NICS indexes indicate the presence of highly aromatic macrocycle and benzene rings while these parameters for pyrrolic ring are significantly smaller than in free pyrrole. The presence of polar solvents practically does not change aromaticity of the ring subunits of the studied compounds.

Keywords Zinc phthalocyanine · Molecular structure · Planarity · HOMA · NICS · DFT · HOMO · LUMO

Introduction

As a result of accidental discoveries [1, 2], metallophthalocyanines (MPcs) have been known for over a century. Since then on, numerous complexes of transition metal ions with phthalocyanine molecule (Pc), which contains eight nitrogen atoms, four pyrrole subunits joined with four azomethine bridges, and four benzene rings, have been commonly used as pigments and dyes [3–7]. Apart from basic research, various phthalocyanine derivatives, including MPcs, have been used as semiconductors, optoelectronic materials, catalysts, and photosensibilizers in photodynamic therapy (PDT) against cancer and as contrast agents in medical diagnostics in magnetic resonance imaging [3–15]. In regard to the latter applications, solubility in water is an important factor for the biologically active compounds [16]. In the case of insoluble compounds, special ways of delivery within patient body are required. However, unsubstituted metallophthalocyanines, including ZnPc, are practically not soluble in water [17]. In this case, the desired solubility could be achieved by introducing several polar groups (for example, carboxylic or sulfonic) to the external benzene rings [18]. The other way of increased water dispersibility, with solubility increased from 16 to 120 mg/l, was recently reported as a result of ZnPc nanowire formation, directly grown from powdered ZnPc [17]. On the other hand, a basic (unsubstituted) ZnPc molecule could be selected as a good computational model, mimicking a less or more distorted structure of its more complex derivatives [18].

Zinc ion is practically not toxic in doses below 225 mg [19], and ZnPc [20–22] (see its general formula in Fig. 1a) is interesting primary due to the fact that Zn(II) ion with d^{10} configuration does not contribute directly to the electronic spectra of phthalocyanine, dominated by transitions within their π-electronic system, formed by several conjugated C=N and C=C double bonds. Thus, reliable prediction of

Electronic supplementary material The online version of this article (https://doi.org/10.1007/s11224-017-1063-3) contains supplementary material, which is available to authorized users.

✉ Teobald Kupka
teobaldk@gmail.com

✉ Małgorzata A. Broda
Malgorzata.Broda@uni.opole.pl

[1] Faculty of Chemistry, University of Opole, 48, Oleska Street, 45-052 Opole, Poland

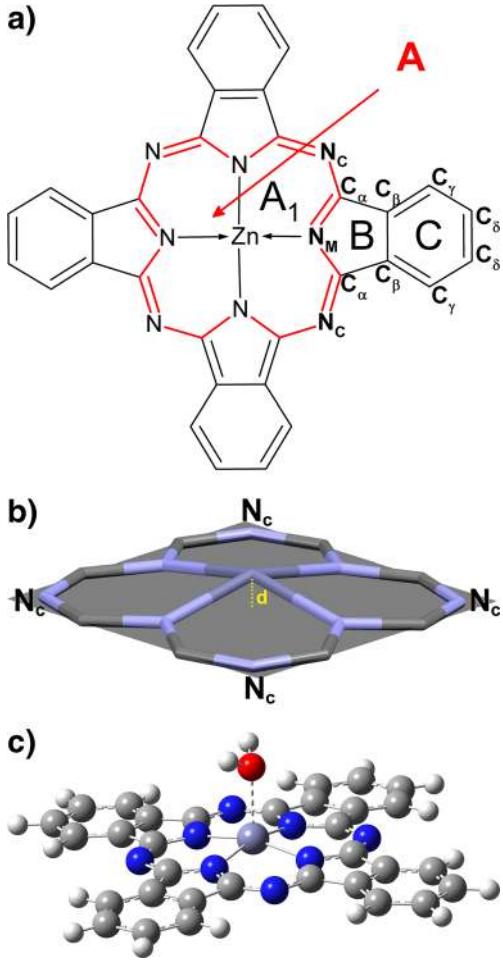

Fig. 1 **a** Schematic structure of zinc phthalocyanine showing atom and ring labeling. **b** Displacement of Zn(II) ion from a plane defined by four N_c atoms (d in Å). **c** The optimized ZnPc·H_2O complex with a single water molecule, axially attached to the metal ion

ZnPc molecular and electronic structure as well as spectroscopic properties could help in designing novel PDT agents [17], including their water-soluble derivatives, and understanding their action, based on photochemical reactions and electronic transitions between the ground and excited states.

For several metal ions, the problem of nonplanarity of their complexes with phthalocyanines was related to the oxidation state of the central atom [22]. Long time ago, the X-ray structure of monohydrated magnesium phthalocyanine (MgPc) [23] showed a significant displacement of metal cation from the molecular plane of the macrocycle (0.496 Å). Similarly, an early X-ray study of the ZnPc complex with *n*-hexylamine as the fifth (axial) ligand [24] indicated a significant displacement of central metal ion from the molecular plane (0.48 Å).

Surprisingly, there are some serious contradictions about the planarity of the ZnPc molecular structure. Thus, in some studies the position of zinc ion with respect to the free (planar) phthalocyanine molecule, observed by X-ray technique [20] and electron diffraction [21], is fixed in the middle of a square formed by four nitrogen atoms (N_c) or, according to other observations, is displaced by about 0.28 Å above the plane formed by them [21] (see Fig. 1a, b). In 1977, using the X-ray technique at room temperature a planar structure of the nonsolvated, centro-symmetric ZnPc molecule crystallized using vacuum sublimation was observed by Scheidt and Dow [20]. The ionic radius of Zn is 0.88 Å [25], thus the Zn ion is tightly located in the middle of four nitrogen atoms and the observed average Zn–N distance is 1.980 Å [20]. Interestingly, in different studies on five coordinated zinc in *n*-hexylamine solvate of ZnPc, a significant displacement (by 0.48 Å) of metal ion from the molecular plane was observed by X-ray [26]. Besides, the Zn–N bonds were markedly longer (2.06 Å). On the other hand, due to their exceptional thermal stability, ZnPc could be sublimated and studied in the gas phase. Later, using the electron diffraction (ED) technique in 1993, gas phase studies at 673 K revealed a nonplanar structure with Zn ion about 0.28 Å above the plane formed by N_c atoms [21]. It is worth mentioning that at this temperature the Zn–N distances were determined fairly accurately (r_e = 1.987 ± 0.013 Å) but the C–C distances in the benzene ring [21] were estimated with high uncertainties [21], ranging from 0.060 to 0.120 Å. Another experimental study in 1999 applied laser-desorption supersonic jet spectroscopy to H_2Pc, ZnPc, and MgPc and concluded that in these molecular systems the macrocycle ring was planar and metal ions were co-planar with the ligand [27].

Molecular modeling [28] using ab initio [29] and density functional theory [30–32] (DFT) also predicts a planar or, in some cases, a "nonplanar (bent)" structure of MPcs. Examples of such molecules, showing different structures, are nonplanar tin phthalocyanine (SnPc) and planar MgPc molecules [22], observed by gas electron diffraction. Liao and Scheiner [33] performed theoretical studies on the electronic structure of complexes, formed by several transition metal ions with porphyrins, porphyrazines, and phthalocyanines. However, a longer discussion on the electronic structure of these molecules is out of scope for the current study.

Due to the size of the ZnPc molecule, as well as the presence of delocalized double bonds and metal ion with d orbitals, the method of choice is DFT with relatively small and incomplete basis sets for its theoretical modeling. In 1999, Fink and co-workers [22] reported on both gas-phase electron diffraction and theoretical DFT studies on the planar equilibrium structure of ZnPc while the BLYP/6-31G* and BLYP/6-31G** data produced a nonplanar molecule with zinc ion about 0.075 Å above the ligand plane [34]. Another experimental electron diffraction and DFT study proposed a planar structure of ZnPc [35]. These authors also obtained a planar D_{4h} structure using B3LYP density functional and large basis sets of 6-311++G** and cc-pVTZ quality.

However, according to our initial studies, the results of such theoretical calculations seem to be strongly sensitive to

the method used and basis set quality. For example, the DFT calculations using a hybrid density functional B3LYP [36–38] combined with 6-31G* basis set are capable to show that in Li_2Pc [39] one lithium cation is below and the other one is above the phthalocyanine ring plane.

Since most theoretical studies [29] concentrate on free molecule in the gas phase, such results neglect the impact of intermolecular interactions in the condensed phases, in particular nonspecific forces due to the presence of solvent molecules. However, implicit modeling of a formation of solute–solvent clusters of different size is more demanding computationally. The simplest model of such solute–solvent system in the current study is ZnPc with a single water molecule directly attached to the metal ion as a fifth ligand (see Fig. 1c). Instead of selecting a discrete model, a simplified treatment of solvent as a dielectric continuum, for example, using a polarizable continuum model (PCM [40]), could provide a significant benefit in terms of computational time and accuracy of ZnPc modeling. Machado and co-workers [41] reported on initial HF and B3LYP studies, combined with a relatively small basis set (6-31G) on ZnPc in DMSO using the PCM approach, and the resulting molecule was planar. However, no such detailed structural studies on ZnPc and ZnPc···H_2O systems using a higher level of theory are available in the literature.

In the case of molecules shaped into ring structures with delocalized electrons from the conjugated double bonds, their (sometimes) structural planarity and bond length averaging results in additional chemical stability, as compared to linear structures with similar number of multiple and single bonds, and is related to the so-called concept of aromaticity [42–49]. A molecular system satisfying specific energetic, geometric, magnetic, and chemical reactivity criteria could be called aromatic [45, 46, 49–54]. Obviously, aromaticity is one of the most frequently used concepts in chemistry. However, unlike chemical bonding, aromaticity is a multidimensional property. Therefore, in common practice are aromaticity studies including results obtained from various criteria [45, 46, 49–54] and recently concentrating on two popular aromaticity indexes: HOMA [45, 46, 52] and NICS [47, 49]. Thus, these parameters should reflect geometrical (HOMA) and magnetic (NICS) properties of three different ring subunits of phthalocyanine (see Fig. 1a).

The harmonic oscillator model of aromaticity (HOMA) is a geometry-based index. The idea behind HOMA [55] is the fact that aromaticity leads to equalization of involved bond lengths. It is calculated as

$$HOMA = 1-\frac{\alpha}{n}\sum_{i=1}^{n}\left(R_{\mathrm{opt}}-R_i\right)^2,$$

where n is the number of bonds in the ring and α is a normalization constant (257.7 for CC and 93.52 for CN bonds). R_{opt} is the optimal bond length (1.388 and 1.334 Å for CC and CN bonds, respectively), which makes HOMA equal to unity for a system with all bonds equal to the optimal ones.

According to Pople and co-workers [56], in a conjugated, monocyclic π-electron system, aromaticity and antiaromaticity are related to the presence of diatropic and paratropic ring currents, respectively. Thus, the NICS index reveals the presence of diatropic or paratropic ring currents. In the molecular structure of phthalocyanines and porphyrins, conjugated rings of different size are present. Therefore, in the current study NICS [49] has been additionally selected as a magnetic criterion of aromaticity in the gas phase and solution. Recently, Junqueira and Dos Santos [57] reported on a very small effect of solvent on aromaticity of benzene. However, they used a fixed, rigid geometry of solute molecule. Both HOMA and NICS were used to determine the aromaticity of the fulvene ring complexed with alkaline metal atoms [58, 59] and in studies on global and local aromaticity in free porphyrins and their complexes with Mg(II) [60]. Thus, determination of these indexes in the current study could provide additional information on the impact of planarity/nonplanarity and solvent effect on ZnPc aromaticity.

In the present theoretical study, we would like to get some insight into the sensitivity of the calculated ZnPc molecular structure, expressed in terms of Zn ion displacement from the plane formed by four nitrogen atoms, in the gas phase and polar solution, to the basis set type and quality. To achieve this aim, two popular and efficient density functionals, B3LYP [36–38] and M06-2X [61, 62], combined with a number of different-quality Pople-type basis sets [63, 64], additionally extended with polarization, diffusion, or both types of additional basis functions, will be applied. It is worth stressing that the energy difference between planar and distorted molecular structures could be fairly small considering the total magnitude of energy of a large ZnPc molecule. Thus, the use of very large integral grid, tight SCF, and geometry optimization criteria should be selected for DFT modeling. Moreover, verifying the presence of positive vibrational frequencies for the obtained structures is also essential. Besides, the use of both planar and distorted structures as starting geometry should be considered. We will concentrate on the calculated values of the d parameter only, e.g., on the planarity of the molecules, and the other structural data will not be considered. Besides, we will calculate the two popular aromaticity indexes, HOMA [45, 46, 52] and NICS [47, 49]. Finally, the highest energy occupied molecular orbital (HOMO) and lowest energy unoccupied molecular orbital (LUMO) energies and their separation [65] (energy gap E_g) for ZnPc and ZnPc···H_2O molecules in the gas phase and polar environment will be estimated and discussed.

Theoretical approach

The structures of ZnPc and ZnPc···H_2O molecules were fully optimized in the gas phase using B3LYP hybrid density functional [36–38], which includes the nonlocal exchange term with three parameters of Becke and the correlation term of

Lee–Yang–Parr, as well as the popular Truhlar's functional M06-2X [61, 62]. Additionally, B3LYP/6-311++G(d,p)-optimized structures of H_2Pc, pyrrole, indole, isoindole, and carbazole were obtained. As starting geometry, a reasonable C_{4v} guess for ZnPc, H_2Pc, and other selected molecules, constructed with the help of GaussView 5.0.8 package [66, 67], was used. In the case of H_2Pc, two different types of pyrrole rings were present: one containing NH and another with N: atom (no hydrogen-bearing nitrogen atom). It is important to underline the fact that optimization of ring structures in our study is less computationally expensive than dealing with flexible molecules possessing a large number of conformations (for example, see the recent experimental and DFT study on glucoside derivatives [68]). All calculations were performed using Gaussian 09 program [66, 67] with tight optimization criteria, SCF = tight, NOSYM keyword, and very accurate grid, specified manually as INT(GRID = 150,590). The presence of true minimum on the hypersurface of energy was confirmed by lack of imaginary frequencies. A selection of systematically changing Pople-type basis sets, including polarization and diffusion functions, was used. Among them were 6-31G, 6-31G(d), 6-31G(d,p), 6-311G(d,p), 6-31+G, 6-31+G(d), 6-31+G(d,p), 6-31++G(d,p), and 6-311++G(d,p).

Modeling of large ZnPc molecular systems is fairly demanding, and in order to show the size of calculations, the number of basis functions and primitive Gaussians was gathered in Table S1 and, for brevity, included in the supplementary material. The solvent effect was included using PCM [40, 66] for modeling DMSO and water impact on the fully optimized structures and aromaticity of the studied molecules. Two different aromaticity indexes, HOMA and NICS, were calculated for the three structural ring subunits of ZnPc and ZnPc···H_2O (see Fig. 1a, c). The NICS calculations at several points in the ZnPc molecule produced a more detailed picture of the ring currents present. Typically, NICS(0) was calculated in the middle of the subunit rings A, A1, B, and C (and directly in the ring plane), but similar results, called NICS(1) and its z-component $NICS(1)_{zz}$, were obtained 1 Å above the molecular plane. The latter parameters are more sensitive to the electronic structure [69]. For comparison, HOMA and NICS values for individual ring subunits of planar H_2Pc, pyrrole, indole, isoindole, and carbazole molecules were calculated. The HOMO and LUMO orbitals, as well as the corresponding E_g energies of ZnPc and ZnPc···H_2O, were directly calculated for the optimized structures.

Results and discussion

Planarity versus nonplanarity of ZnPc molecular structure

A simplified structural formula of planar ZnPc is shown in Fig. 1a. Due to its D_{4h} symmetry, only selected atoms and three different ring subunits, belonging to one fourth of the molecule, are labeled. This situation is similar to that in the Mg complex with porphyrins [60]. In contrast, in free H_2P molecules two distinct types of rings 1, 3 and 2, 4 were revealed from HOMA and NICS indexes [60].

The large inner macrocycle, as well as the five- and six-membered rings of ZnPc are labeled in Fig. 1a with bold letters A, B, and C. Moreover, the nitrogen atoms bonded to metal ion and carbon atoms are labeled N_m and N_c, respectively. As mentioned in the "Introduction" section, we are mainly interested in parameter d, which indicates the deviation (displacement or pulling up, shown in Fig. 1b) of zinc ion from the plane formed by four N_c atoms. For structures, characterized by $d > 0$, the ligand molecule is nonplanar. In such case, the Pc molecular fragment is slightly shaped in a form of a cone or saucer [22]. For brevity, the Cartesian coordinates of fully optimized ZnPc and ZnPc···H_2O structures at the B3LYP/6-311++G(d,p) and M06-2X/6-311++G(d,p) levels of theory are included in Tables S2–S7 in the supplementary material.

In Table 1 are gathered values of parameter d, obtained from ZnPc geometry optimization in the gas phase, DMSO, and water using B3LYP and M06-2X density functionals combined with basis sets, containing polarization and diffuse functions. It is important to notice a planar structure of ZnPc in the gas phase (d = 0.000 Å) predicted by both density functionals and all basis sets used. The situation dramatically changes in the presence of polar solvents. Thus, in DMSO solution, B3LYP combined with small Pople-type basis sets, e.g., 6-31G, 6-31G(d) and 6-31G(d,p), predicts a significant displacement of zinc ion from the plane formed by four N_c atoms (by 0.300 to 0.330 Å). Somehow, smaller d values (from 0.220 to 0.284 Å) are observed in the presence of water for all basis sets lacking diffuse functions. Augmenting the Pople basis sets with diffuse functions leads to the planar structures of ZnPc in DMSO and water. M06-2X functional predicts a nonplanar structure of ZnPc in DMSO (d changes from 0.260 to 0.398 Å), and the only planar geometries are obtained using 6-311G(d,p) and 6-31+G basis sets. In addition, M06-2X produces nearly all bent structures in water (d from 0.283 to 0.400 Å) and the only planar complex is calculated with 6-31+G basis set (Table 2).

The diffuse functions are very important for calculations of molecular systems involving double bonds and lone electron pairs. For example, using DFT and MP2 methodology combined with basis sets containing (or lacking) polarization and diffuse functions [73], we also noticed the impact of a basis set on the predicted planarity/pyramidalization of NH_2 group in free formamide molecule. It is apparent in the current study from Table 1 that, in contrast to B3LYP, the M06-2X calculations with basis sets containing polarization and diffuse functions are capable of predicting a nonplanar structure of the ZnPc complex in a polar environment. The Zn(II) with ionic

Table 1 The calculated distance d (in Å) between the zinc ion and the plane, defined by four nitrogen atoms (N_c) in ZnPc

Basis set	B3LYP			M06-2X		
	Gas phase	DMSO	Water	Gas phase	DMSO	Water
6-31G	0.000	0.300	0.220	0.000	0.359	0.361
6-31G(d)	0.000	0.330	0.245	0.071	0.398	0.400
6-31G(d,p)	0.000	0.330	0.245	0.071	0.398	0.400
6-311G(d,p)	0.000	0.000	0.248	0.000	0.000	0.311
6-31+G	0.000	0.000	0.000	0.000	0.000	0.000
6-31+G(d)	0.000	0.000	0.000	0.000	0.260	0.283
6-31+G(d,p)	0.000	0.000	0.000	0.000	0.260	0.283
6-31++G(d,p)	0.000	0.000	0.000	0.000	0.263	0.284
6-311++G(d,p)	0.000	0.000	0.000	0.000	0.268	0.288
Lit.	0.00[a]; 0.00[b]; 0.00[c]; 0.075[d]; 0.00[e];					
Exp.	0.00[f]; 0.28[g]; 0.00[h]; 1.0[i]; 0.00[j]; 0.00[k]; 0.00[l]					

[a] B3LYP/6-311++G(2d,2p) result from [70]

[b] HF, B3LYP, and MP2 with 6-31G* result from [41]

[c] UB3LYP/6-31G(d,p) data for ZnPc, from [71]

[d] B3LYP/6-31G** data from [34]

[e] B3LYP/6-31G* data for ZnPc, from [72]

[f] X-ray data for ZnPc, from [20]

[g] ED data from [21]

[h] Reinvestigation of ED data from [22]

[i] ED data for SnPc, from [22]

[j] ED data for MgPc, from [22]

[k] Laser-desorption supersonic jet spectroscopy data for H2Pc with D_{2h} symmetry; planar are also MgPc and ZnPc with D_{4h} symmetry, from [27]

[l] ED data from [35]

radius of 0.88 Å is very tightly accommodated in the middle of the plane formed by the four nearest N atoms, and the M06-2X/6-31+G(d) distance between zinc ion and the nearest nitrogen atom is 2.000 Å. Therefore, nonspecific interactions with polar solvents are able to remove zinc ion from the cavity. The M06-2X results shown in Table 1 indicate that polar solvents pull up Zn(II) ion by about 0.3 Å over the plane formed by four nitrogen atoms and could lead to five (but not six) coordinated central metal ions.

Structural feature of the ZnPc···H_2O complex

In Table 2 are gathered B3LYP and M06-2X calculated displacements (d) of zinc ion in the axially monohydrated ZnPc···H_2O complex from a plane formed by four N_c atoms. The displacement in water for three selected basis sets (6-31G(d,p), 6-31+G(d,p), 6-311++G(d,p)) is bigger by 0.12 to 0.36 Å than calculated for the nonhydrated ZnPc complex. In this case, the M06-2X density functional also produces, in almost all cases, a more significant nonplanarity than B3LYP (d larger by about 0.01 to 0.06 Å). As for ZnPc, the presence of diffuse functions in basis sets decreases the nonplanarity of the phthalocyanine macrocycle. It is worth mentioning that the recent X-ray studies [26] on three axial ZnPc···*n*-alkylamines nicely agree with our data and prove the existence of similar nonplanar structures with d parameter of about 0.5 Å. In addition, the subsequent B3LYP/6-31+G(d)

Table 2 The distance d (in Å) between the zinc ion and the plane defined by four nitrogen atoms (N_c) in the axially monohydrated ZnPc···H_2O complex, calculated with B3LYP and M06-2X density functionals and selected basis sets

Basis set	B3LYP		M06-2X	
	Gas phase	Water	Gas phase	Water
6-31G(d,p)	0.461	0.493	0.448	0.518
6-31+G(d,p)	0.315	0.359	0.364	0.402
6-311++G(d,p)	0.328	0.364	0.367	0.418
Lit.[a]	0.428; 0.428; 0.429			
Exp.	0.494[b]; 0.498[b]; 0.477[b]; 0.38[c]; 0.496[d]; 0.48[e]			

[a] B3LYP/6-31+G(d) result for three ZnPc···*n*-alkylamines, from [26]

[b] X-ray data result for three ZnPc···*n*-alkylamines, from [26]

[c] X-ray data for ZnPc···H_2O···DMF_2, from [74]

[d] X-ray data for MgPc···H_2O, from [75]

[e] X-ray data for ZnPc···*n*-hexylamine, from [24]

calculations by these authors [26] closely reproduced the observed crystal structure of these solvates (d was about 0.43 Å). For completeness, the Cartesian coordinates of fully optimized ZnPc and ZnPc···H_2O structures at the B3LYP/6-311++G(d,p) and M06-2X/6-311++G(d,p) levels of theory are included in Tables S2–S7 in the supplementary material.

Aromaticity of different structural fragments of ZnPc and ZnPc···H_2O

The presence of conjugated double bonds in rings of different shape and size could lead to electron delocalization and specific aromaticity in various structural subunits of phthalocyanines and their derivatives. As a result, this could lead to different degree of bond length equilibration and planarity due to the preferred p_z orbital overlapping. Thus, the HOMA index seems to be a proper structural measure of aromaticity and NICS should probe the induced magnetic properties resulting from ring currents due to electron delocalization in the external magnetic field.

The B3LYP/6-311++G(d,p) and M06-2X/6-311++G(d,p) calculated HOMA values for the ZnPc molecule subunits in the gas phase, DMSO, and water using selected basis sets are shown in Fig. 2. For brevity, the calculated HOMA values with all used basis sets are gathered in Table S8 in the supplementary material. It is apparent from Fig. 2 that both density functionals predict nearly the same HOMA values for the corresponding ZnPc subunits. However, the values calculated with the B3LYP functional are negligibly smaller (by about 0.01) than the corresponding M06-2X ones. In particular, the inner, 16-membered macrocyclic ring A and outer benzene subunit C indicate their very high aromaticity (the HOMA index close to 1 is similar to the aromaticity of a reference compound, e.g., benzene). In contrast, the five-membered pyrrolic ring B is significantly less aromatic than free pyrrole (HOMA value is about 0.33 instead of 0.87). In addition, the presence of polar solvents results in a very small increase of the HOMA index.

Looking closer at the B3LYP-calculated HOMA values in Table S8, we notice that enlarging a small basis set 6-31G with polarized and diffuse functions and forming more complete 6-311G(d,p) or 6-311++G(d,p) ones results in an increase in the corresponding values for A subunit from about 0.87 to 0.94 (gas phase), from 0.88 to 0.95 (DMSO), and from 0.91 to 0.97 (water). The presence of a polar solvent also slightly increases HOMA values of macrocycle A (by about 0.01 to 0.02). In the case of benzene subunits, an increase of the HOMA index by 0.02 to 0.03 is observed upon using a more complete and flexible basis set 6-311++G(d,p), in comparison to a small 6-31G one. The water-to-gas shift of the HOMA index is also very small (0.02). Interestingly, the calculated HOMA values for subunit B are more sensitive to the basis set quality (0.30 in the gas phase increases to 0.38, as obtained with 6-31G and 6-311++G(d,p) basis sets). Besides, moving from the gas phase to DMSO and water we observe an irregular change of the HOMA index—from 0.38 to 0.34 and 0.40. This inconsistent pattern of HOMA changes due to solvent effect, modeled by a simple PCM, could also indicate that such calculations may not be sufficient to reliably predict small changes of aromaticity. The M06-2X-calculated HOMA index changes are very similar to those obtained with B3LYP density functional and the selected basis sets.

It is interesting to compare HOMA values of structural subunits in ZnPc and ZnPc···H_2O in a different environment,

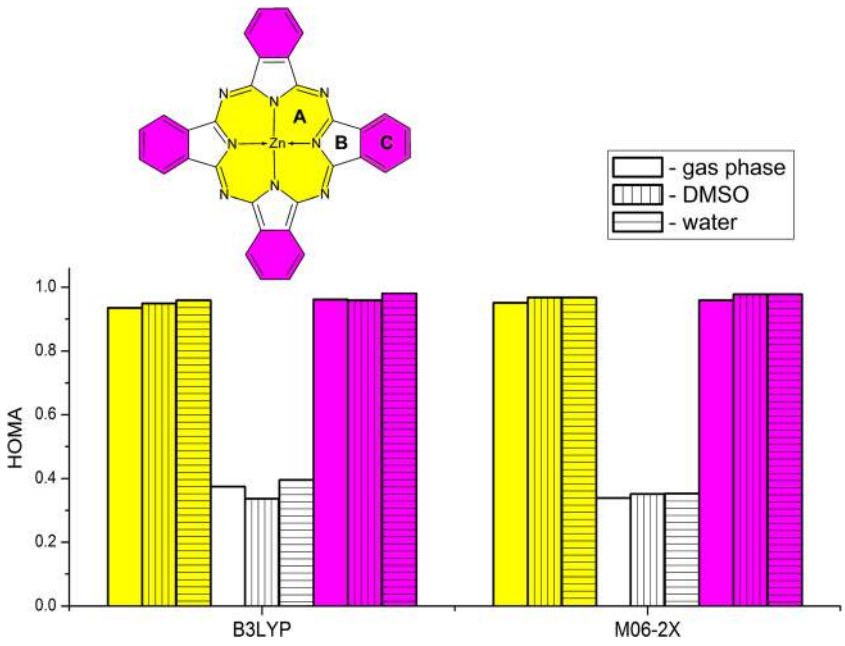

Fig. 2 B3LYP/6-311++G(d,p)- and M06-2X/6-311++G(d,p)-calculated HOMA indexes for ZnPc ring subunits A, B, and C (marked in yellow, white, and magenta) in the gas phase, DMSO, and water

Table 3 B3LYP/6-311++G(d,p)-calculated HOMA values in the gas phase and water for the three ring subunits in ZnPc and ZnPc···H_2O and for two reference molecules (benzene and pyrrole)

Molecule	A		B		C	
	Gas phase	Water	Gas phase	Water	Gas phase	Water
ZnPc	0.935	0.959	0.375	0.396	0.961	0.981
ZnPc···H_2O	0.945	0.953	0.352	0.326	0.960	0.959
Benzene	–	–	–	–	0.987	0.984
Pyrrole	–	–	0.865	0.858	–	–

as well as with benzene and pyrrole, used as aromaticity references (see Table 3). It is apparent that the macrocycle A in ZnPc and ZnPc···H_2O is highly aromatic. Thus, HOMA calculated in vacuum for subunit A in these molecules is in the range of 0.95 and is close to benzene (HOMA of 0.99). Interestingly, no significant difference of HOMA upon changing from planar ZnPc to a distorted structure of ZnPc···H_2O is observed (difference of 0.01 only). The increase of HOMA as a result of calculations in water is also negligible (about 0.01–0.02) for both molecules. HOMA values for subunit C indicate it aromaticity being comparable to free benzene (0.99), and the corresponding change in the presence of water is negligible (0.01–0.02). However, the HOMA value of subunit B is about two times smaller than in free pyrrole (0.38 vs. 0.87 in vacuum). All calculated HOMA values with both density functionals and selected basis sets for ZnPc···H_2O are gathered in Table S9. From the above, it follows that the presence of polar solvent has no impact on HOMA index in these closely related molecules.

Magnetic criteria of aromaticity, including NICS (0), NICS (1), and NICS $(1)_{zz}$, for selected subunits of ZnPc and ZnPc···H_2O molecules in the gas phase, DMSO, and water were calculated using both density functionals and selected basis sets. It is important to mention here that the aromaticity of a ring could be also affected by its size, for example, to change due to interaction with the solvent. The zz-component seems to be the most sensitive parameter, and therefore in Table 4 are shown B3LYP- and M06-2X-calculated NICS $(1)_{zz}$ values for the three ring subunits of ZnPc in the gas phase, DMSO, and water using selected basis sets. The A1 subunit is now selected as one fourth of the initial ring A, and it includes zinc ion at one corner (see Fig. 3). It is apparent from Table 4 that B3LYP-calculated NICS$(1)_{zz}$ of − 31.2 ppm in the gas phase for this six-membered ring changes to − 36.6 and − 35.3 ppm with an enlarging initial 6-31G basis set to 6-31G(d,p) and 6-311++G(d,p). The corresponding values of NICS $(1)_{zz}$, predicted with M06-2X density functional, behave in a similar manner (an increase from − 34.3 to − 39.8

Table 4 The B3LYP- and M06-2X-calculated NICS $(1)_{zz}$ values (in ppm) for three ring subunits of ZnPc in the gas phase, DMSO, and water using selected basis sets

Basis set	A1			B			C		
	Gas phase	DMSO	Water	Gas phase	DMSO	Water	Gas phase	DMSO	Water
B3LYP									
6-31G	− 31.24	− 29.71	− 30.04	− 4.93	− 3.05	− 3.99	− 23.32	− 22.64	− 23.15
6-31G(d)	− 35.47	− 33.71	− 34.02	− 6.74	− 4.69	− 5.70	− 25.98	− 25.25	− 25.81
6-31G(d,p)	− 35.51	− 33.76	− 34.07	− 6.77	− 4.73	− 5.74	− 26.07	− 25.34	− 25.90
6-311G(d,p)	− 36.33	− 36.41	− 34.52	− 6.17	− 5.32	− 4.47	− 25.73	− 25.43	− 25.33
6-31+G	− 31.10	− 31.20	− 31.20	− 5.06	− 4.20	− 4.22	− 23.05	− 22.76	− 22.81
6-31+G(d)	− 35.21	− 35.39	− 35.39	− 6.82	− 5.93	− 5.95	− 25.62	− 25.32	− 25.35
6-31+G(d,p)	− 35.25	− 35.43	− 35.43	− 6.83	− 5.96	− 5.99	− 25.70	− 25.39	− 25.42
6-31++G(d,p)	− 35.27	− 35.45	− 35.46	− 6.79	− 5.98	− 5.95	− 25.74	− 25.37	− 25.37
6-311++G(d,p)	− 35.34	− 35.52	− 35.48	− 6.79	− 5.92	− 5.96	− 25.74	− 25.43	− 25.51
M06-2X									
6-31G	− 34.25	− 32.10	− 31.81	− 6.29	− 3.84	− 4.59	− 24.55	− 23.62	− 23.97
6-31G(d)	− 39.32	− 36.26	− 35.82	− 8.21	− 5.00	− 5.80	− 27.39	− 26.17	− 26.56
6-31G(d,p)	− 39.36	− 36.30	− 35.86	− 8.24	− 5.04	− 5.83	− 27.47	− 26.25	− 26.64
6-311G(d,p)	− 39.76	− 39.82	− 37.23	− 7.12	− 6.17	− 5.02	− 26.98	− 26.72	− 26.38
6-31+G	− 34.05	− 34.20	− 34.17	− 6.42	− 5.45	− 5.45	− 24.36	− 24.08	− 24.08
6-31+G(d)	− 38.58	− 36.87	− 36.37	− 7.93	− 5.53	− 6.22	− 26.93	− 26.07	− 26.40
6-31+G(d,p)	− 38.60	− 36.89	− 36.40	− 7.95	− 5.55	− 6.25	− 27.00	− 26.13	− 26.46
6-31++G(d,p)	− 38.62	− 36.88	− 36.40	− 7.96	− 5.55	− 6.24	− 26.97	− 26.11	− 26.45
6-311++G(d,p)	− 38.65	− 36.77	− 36.31	− 7.85	− 5.46	− 6.10	− 27.02	− 26.09	− 26.44

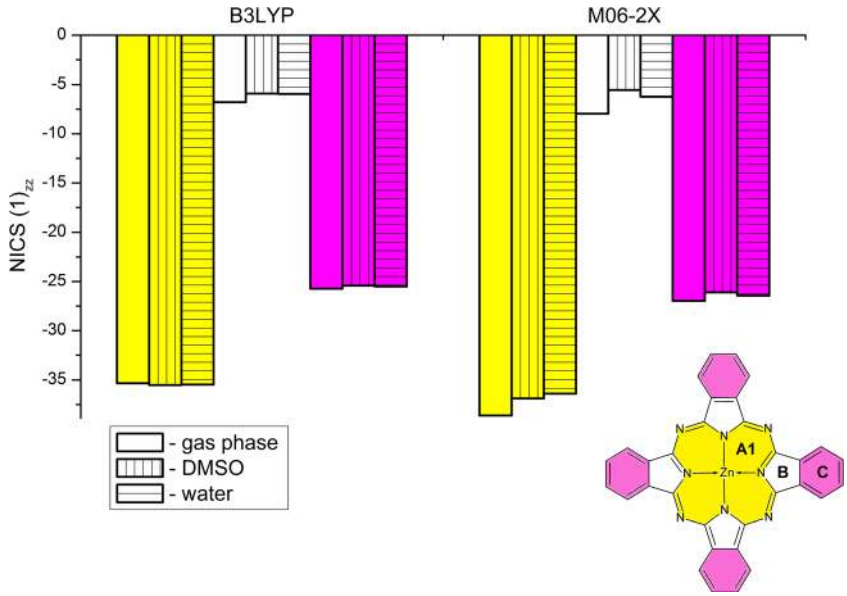

Fig. 3 The B3LYP/6-311++G(d,p)- and M06-2X/6-311++G(d,p)-calculated NICS(1)$_{zz}$ index (in ppm) for three ring subunits of ZnPc in the gas phase, DMSO, and water

and − 38.6 ppm is observed). On the other hand, concluding from B3LYP/6-311++G(d,p) results, the presence of polar solvent does not influence the aromaticity of A1 subunit (− 35.3 in vacuum increases to only − 35.5 ppm in water).

The NICS(1)$_{zz}$ index for the C ring in vacuum (− 23.3 ppm), calculated at the B3LYP/6-31G level of theory, is by about 2.4 ppm less aromatic than that determined with a larger basis set of 6-311++G(d,p). The latter value decreases by about 0.2 ppm in the presence of water. The five-membered ring B shows a very low aromaticity and it also becomes more aromatic when increasing the initial 6-31G basis set to 6-311++G(d,p), and the corresponding B3LYP-calculated NICS(1)$_{zz}$ parameter changes from − 4.9 to − 6.8 ppm. The relative aromaticity of ring subunits A1, B, and C, expressed by the NICS(1)$_{zz}$ parameter, is similar to earlier reported properties of these rings in free molecule of silicon phthalocyanine (compare NICS(0) and NICS(1) values in [76]) and magnesium phthalocyanine [77]. Interestingly, in germanium phthalocyanines [77], NICS(1) predicted the presence of anti-aromatic rings. In this molecule, ring B was the most, and ring C the least, anti-aromatic.

It is also apparent from Fig. 3 that both density functionals, combined with the 6-311++G(d,p) basis set, predict similar trends in NICS(1)$_{zz}$ values in the gas phase, DMSO, and water for the corresponding ZnPc subunits. However, in this case the aromaticity of A1, B, and C subunits differs more than in the case of HOMA parameters. In addition, more distinct changes (decrease) of aromaticity due to the presence of polar solvent are clearly seen.

All calculated NICS(1)$_{zz}$ values with both density functionals and selected basis sets for ZnPc···H_2O are gathered in Table S9. It is interesting to compare the B3LYP/6-311++G(d,p)-predicted NICS(1)$_{zz}$ values of structural subunits in ZnPc and ZnPc···H_2O molecules in different environments with benzene and pyrrole (see Table 5). First, according to NICS(1)$_{zz}$ calculations, a very high aromaticity of subunit A1 for ZnPc and ZnPc···H_2O in vacuum and water is clearly demonstrated (about − 35 ppm, a value larger than for free benzene and pyrrole). In contrast, the benzene-like ring C is markedly less aromatic than the parent benzene (about - 25 vs. − 29 ppm). Finally, a very low aromaticity of ring B with respect to free pyrrole is observed (about − 7 to − 4 vs. − 31 ppm). Formation of monohydrated ZnPc from the free ZnPc complex slightly decreases the aromaticity of A1, B, and C rings (by 1.6, 2.3, and 3.6 in the gas phase and 1.8, 2.1, and 1.0 ppm in water). Moreover, no significant changes

Table 5 B3LYP/6-311++G(d,p)-calculated NICS(1)$_{zz}$ values in the gas phase and water for three ring subunits of ZnPc and ZnPc···H_2O and for the reference molecules (benzene and pyrrole)

Molecule	A1		B		C	
	Gas phase	Water	Gas phase	Water	Gas phase	Water
ZnPc	− 35.339	− 35.484	− 6.789	− 5.963	− 25.737	− 25.512
ZnPc···H_2O	− 33.738	− 33.664	− 4.549	− 3.932	− 24.990	− 24.535
Benzene	–	–	–	–	− 29.253	− 29.226
Pyrrole	–	–	− 31.004	− 31.120	–	–

Table 6 B3LYP/6-311++G(d,p)-calculated HOMA and NICS values for selected five-membered rings containing nitrogen

Molecule	HOMA		NICS(0)		NICS(1)		$NICS(1)_{zz}$	
Carbazole	0.604		− 9.2375		− 8.4581		− 21.1073	
Indole	0.713		− 12.420		− 10.184		− 28.681	
Isoindole	0.753		− 16.237		− 12.783		− 37.941	
Pyrrole	0.854		− 13.6358		− 10.0821		− 31.004	
H_2Pc	0.535[a]	0.378[b]	− 4.378[a]	3.963[b]	−6.190[a]	−1.497[b]	−14.090[a]	1.155[b]
ZnPc	0.375		− 0.601		− 4.451		− 6.789	
R^2			0.87844[a]; 0.88803[b]		0.77427[a]; 0.81309[b]		0.85372[a]; 0.87953[b]	

of those rings aromaticity, caused by polar solvent for ZnPc and ZnPc···H_2O, are visible (predicted water-to-gas shifts are small).

It is also important to look for some correlations between HOMA and NICS indexes of local aromaticity for the ZnPc molecule. For brevity, in the supplementary material are gathered B3LYP- and M06-2X-calculated $NICS(1)_{zz}$ values for rings A, B, and C in the gas phase, DMSO, and water using 6-311++G(d,p) basis set (Figs. S1A and S1B). As expected, there is some correlation for data clusters showing low and high aromaticity. However, one could describe it as a kind of weak linear dependence only (R^2 of about 0.87 and 0.86 for B3LYP and M06-2X results were predicted).

Another important aspect of aromaticity of five- and six-membered units of ZnPc is related to very low values of both types of aromaticity indexes in case of pyrrole unit. To shed more light on this topic, several arbitrarily selected ring structures containing nitrogen atom were additionally analyzed. HOMA and NICS values for selected five- and six-membered rings are gathered in Table 6. In the case of five-membered rings (Table 6) a relatively weak correlation (R^2 from 0.77 to 0.89) is observed between those two different indexes of aromaticity. In addition, rings containing the NH fragment are slightly less aromatic (R^2 from 0.77 to 0.88) than rings containing N: (R^2 from 0.81 to 0.89). From the data gathered in Table 6, it is apparent that conjugation of pyrrole unit with one or two benzene rings decreases its initial aromaticity. This change is most pronounced for H_2Pc and ZnPc (see also Fig. S2A and S2AA in the supplementary material). Only in the case of isoindole is the aromaticity of the five-membered ring higher than for the free-standing pyrrole.

On the other hand, there is apparently no correlation between NICS and HOMA values in the case of highly aromatic six-membered rings conjugated to five-membered heterocycles containing nitrogen (see Table 7 and Fig. S2B or S2BB with very small values of R^2). These data could also point at the multidimensional character of aromaticity in the studied molecular systems.

[a]Containing the NH pyrrole subunit

[b]Containing the N: pyrrole subunit

Some fairly weak linear correlations between the aromatic indexes calculated for individual ring subunits of ZnPc in the gas phase, DMSO, and water are also observed. For example, B3LYP/6-311++G(d,p)-calculated R^2 values for linear correlations of HOMA indexes for ratio B vs. A and C vs. A are 0.47521 and 0.67486, respectively (Fig. S3A). Interestingly, a higher R^2 is observed for similar correlation of HOMA values for ring C vs. B (R^2 is 0.87615, see Fig. S3B).

HOMO, LUMO, and Eg energies

In the last step of our study, we analyze the HOMO/LUMO energy gap of ZnPc and ZnPc···H_2O in vacuum, DMSO, and water. In this case, the decreased energy gap (E_g in eV) will correspond to the increase in chemical reactivity.

Table 7 B3LYP/6-311++G(d,p)-calculated HOMA and NICS values for selected six-membered rings conjugated with five-membered heterocyclic rings containing nitrogen

Molecule	HOMA		NICS(0)		NICS(1)		$NICS(1)_{zz}$	
Isoindole	0.644		− 6.623		− 8.523		− 22.991	
Indole	0.918		− 9.710		− 10.827		− 29.637	
Carbazole	0.943		− 9.5346		− 10.6559		− 28.7275	
Benzene	0.989		− 8.066		− 10.229		− 29.253	
H_2Pc	0.968[a]	0.988[b]	− 8.148[a]	− 6.667[b]	−9.950[a]	−8.690[b]	−27.708[a]	−23.792[b]
ZnPc	0.961		− 7.518		− 9.757		− 25.736	
R^2			0.31409; 0.11868		0.6274; 0.24551		0.28618; 0.27315	

[a] Containing the NH pyrrole subunit

[b] Containing the N: pyrrole subunit

Table 8 B3LYP- and M06-2X-calculated HOMO and LUMO energies and energy gaps (in eV) using selected basis sets for ZnPc

Basis set	Gas phase			DMSO			Water		
	HOMO	LUMO	E_g	HOMO	LUMO	E_g	HOMO	LUMO	E_g
B3LYP									
6-31G	− 5.118	− 2.877	2.241	− 5.222	− 2.981	2.241	− 5.229	− 2.987	2.243
6-31G(d)	− 4.939	− 2.751	2.188	− 5.022	− 2.835	2.187	− 5.031	− 2.842	2.189
6-31G(d,p)	− 4.946	− 2.758	2.188	− 5.026	− 2.838	2.188	− 5.035	− 2.845	2.190
6-311G(d,p)	− 5.161	− 2.983	2.178	− 5.237	− 3.048	2.189	− 5.228	− 3.039	2.189
6-31+G	− 5.367	− 3.153	2.213	− 5.445	− 3.231	2.214	− 5.446	− 3.231	2.215
6-31+G(d)	− 5.225	− 3.066	2.159	− 5.290	− 3.129	2.161	− 5.290	− 3.128	2.162
6-31+G(d,p)	− 5.232	− 3.073	2.159	− 5.294	− 3.132	2.162	− 5.294	− 3.131	2.163
6-31++G(d,p)	− 5.233	− 3.073	2.159	− 5.294	− 3.132	2.162	− 5.295	− 3.132	2.162
6-311++ G(d,p)	− 5.271	− 3.112	2.158	− 5.340	− 3.177	2.163	− 5.343	− 3.180	2.163
M06-2X									
6-31G	− 5.901	− 2.364	3.536	− 6.011	− 2.472	3.539	− 6.012	− 2.473	3.539
6-31G(d)	− 5.720	− 2.255	3.464	− 5.807	− 2.341	3.466	− 5.809	− 2.342	3.466
6-31G(d,p)	− 5.720	− 2.256	3.465	− 5.806	− 2.340	3.466	− 5.808	− 2.342	3.466
6-311G(d,p)	− 5.887	− 2.451	3.436	− 5.986	− 2.537	3.449	− 5.969	− 2.519	3.450
6-31+G	− 6.094	− 2.596	3.498	− 6.189	− 2.689	3.501	− 6.189	− 2.686	3.503
6-31+G(d)	− 5.949	− 2.526	3.423	− 6.020	− 2.592	3.428	− 6.019	− 2.591	3.428
6-31+G(d,p)	− 5.950	− 2.526	3.423	− 6.019	− 2.592	3.427	− 6.018	− 2.590	3.428
6-31++G(d,p)	− 5.950	− 2.526	3.423	− 6.019	− 2.591	3.428	− 6.017	− 2.590	3.428

In Tables 8 and 9 are gathered B3LYP- and M06-2X-calculated HOMO and LUMO energies and E_g for ZnPc and ZnPc···H_2O. In this case, the improvement of the basis set quality from 6-31G to 6-311++G(d,p) results in a very small energy gap change (a decrease of the B3LYP-predicted values by about 0.1 eV in the gas phase). The results obtained for ZnPc and ZnPc···H_2O are very similar. Moreover, there is no visible solvent impact on E_g. The corresponding tendencies observed for M06-2X energy parameters (the absolute magnitudes of E_g are about 1.2 eV higher in comparison to B3LYP) are similar to those calculated with the B3LYP density functional. Our B3LYP-calculated gap energy values in the gas phase and shown in Tables 8 and 9 nicely reproduce the recently reported B3LYP/6-31G* value (2.188 eV is practically the same as the literature value of 2.19 eV), and our best result, calculated with the 6-311++G** basis set, is 2.158 eV.

Conclusions

The planarity of ZnPc and ZnPc···H_2O structures and aromaticity of their ring subunits were systematically studied by DFT methods in the gas phase and solution, modeled by the PCM method, using basis sets of different quality. According

Table 9 B3LYP- and M06-2X-calculated HOMO and LUMO energies and energy gaps (in eV) using selected basis sets for ZnPc···H_2O

Basis set	Gas phase			DMSO			Water		
	HOMO	LUMO	E_g	HOMO	LUMO	E_g	HOMO	LUMO	E_g
B3LYP									
6-31G(d,p)	− 4.791	− 2.592	2.199	− 4.972	− 2.781	2.191	− 4.975	− 2.784	2.191
6-31+G(d,p)	− 5.110	− 2.937	2.173	− 5.241	− 3.077	2.164	− 5.245	− 3.081	2.164
6-311++ G(d,p)	− 5.143	− 2.971	2.172	− 5.287	− 3.122	2.165	− 5.291	− 3.126	2.165
M06-2X									
6-31G(d,p)	− 5.554	− 2.075	3.479	− 5.759	− 2.290	3.468	− 5.762	− 2.294	3.468
6-31+G(d,p)	− 5.814	− 2.373	3.441	− 5.973	− 2.543	3.431	− 5.975	− 2.544	3.431
6-311++ G(d,p)	− 5.837	− 2.408	3.429	− 6.005	− 2.586	3.419	− 6.009	− 2.590	3.419

to our best knowledge, these are the first so extensive studies on the impact of basis set quality and environment on the structural and magnetic properties of free zinc phthalocyanine and its monohydrated complex.

Both B3LYP and M06-2X density functional calculations predict a planar structure of the ZnPc molecule in the gas phase for all basis sets used. The presence of polar environment, modeled by the PCM method, in most cases results in displacement of zinc ion from the ligand plane by about 0.2 to 0.4 Å. However, in the case of B3LYP density functional combined with selected basis sets, additionally augmented with diffuse functions, a planar structure is observed. The displacement of zinc ion calculated with Truhlar's functional, in comparison to B3LYP, is typically larger by about 0.1 to 0.15 Å.

In contrary, a nonplanar structure of the ZnPc···H_2O monohydrated complex, with d ranging from 0.3 to 0.5 Å in the gas phase and water, is calculated by DFT. The presence of polar surrounding increases the displacement of zinc ion only slightly (by about 0.03 Å). These results nicely reproduce available experimental data.

Both HOMA and NICS$(1)_{zz}$ indexes, calculated with B3LYP and M06-2X density functionals, predict high aromaticity of subunits A1 and C in both ZnPc and ZnPc···H_2O for all basis sets used. In contrast, the five-membered ring B shows a significantly lower aromaticity in comparison to free pyrrole (B3LYP/6-311++G(d,p)-calculated HOMA in the gas phase is 0.38 vs. 0.87 for a reference molecule). This is additionally supported by a magnetic index of aromaticity (B3LYP/6-311++G(d,p)-calculated NICS$(1)_{zz}$ in the gas phase is −6.8 vs. −31.0 ppm for a reference molecule). No significant impact of polar solvent on aromaticity was observed.

Based on linear correlations for individual subunits, HOMA and NICS indexes of ZnPc could be considered as complementary tools, capable to study its local aromaticity.

The calculated HOMO, LUMO, and E_g energies for ZnPc and ZnPc···H_2O are not sensitive to basis set quality or presence of polar solvent. However, the absolute values of E_g calculated with M06-2X density functional are about 1 eV larger than those predicted by B3LYP.

Acknowledgments Calculations were carried out in Wrocław Centre for Networking and Supercomputing (http://www.wcss.wroc.pl), and in the Academic Computer Centre, CYFRONET, AGH, Kraków. T. K. and M. B. were supported by a project from the Faculty of Chemistry, University of Opole.

Compliance with ethical standards

Ethical statement All ethical guidelines have been adhered.

Conflict of interest The authors declare that they have no conflict of interest.

References

1. Braun A, Tcherniac J (1907) Über die Produkte der Einwirkung von Acetanhydrid auf Phthalamid. Ber Dtsch Chem Ges 40(2):2709–2714. https://doi.org/10.1002/cber.190704002202
2. de Diesbach H, von der Weid E (1927) Quelques sels complexes des o-dinitriles avec le cuivre et la pyridine. Helv Chim Acta 10(1):886–888. https://doi.org/10.1002/hlca.192701001110
3. Moser FH, Thomas AL (1963) Phthalocyanine compounds. Reinhold, New York
4. Moser FH, Thomas AL (1983) The phthalocyanines. CRC Press, Boca Raton
5. Thomas AL (1990) Phthalocyanine research and applications. CRC Press, Boca Raton
6. Leznoff CC (1989) 1993 and 1996 Phthalocyanines: properties and applications, vol 1–4. VCH Publishers, New York
7. McKeown NB (1998) Phthalocyanine materials: synthesis, structure and function. Cambridge University Press, Cambridge
8. Batey J, Petty MC, Roberts GG, Wright DR (1984) GaP/phthalocyanine Langmuir-Blodgett film electroluminescent diode. Electron Lett 20:489–491
9. Snow AW, Barger WR, Klusty M, Wohltjen H, Jarvis NL (1986) Simultaneous electrical conductivity and piezoelectric mass measurements on iodine-doped phthalocyanine Langmuir-Blodgett films. Langmuir 2:513–519
10. Bardin M, Bertounesque E, Plichon V, Simon J, Ahsen V, Bekaroglu O (1989) Electrochemistry of lutetium crowned ether diphthalocyanine films. J Electroanal Chem 271:173–180
11. Loutfy RO, Sharp JH, Hsiao CK, Ho R (1981) Phthalocyanine organic solar cells: indium/x-metal free phthalocyanine Schottky barriers. J Appl Phys 52:5218
12. Kerp HR, Faassen EEV (2000) Effects of oxygen on exciton transport in zinc phthalocyanine layers. Chem Phys Lett 332:5–12
13. Lukyanets EA (1999) Phthalocyanines as photosensitizers in the photodynamic therapy of cancer. J Porphyrins Phthalocyanines 3:424
14. Bonnett R (1995) Photosensitizers of the porphyrin and phthalocyanine series for photodynamic therapy. Chem Soc Rev 24:19–33
15. Aydın Tekdaş D, Garifullin R, Şentürk B, Zorlu Y, Gundogdu U, Atalar E, Tekinay AB, Chernonosov AA, Yerli Y, Dumoulin F, Guler MO, Ahsen V, GA G (2014) Design of a Gd-DOTA-phthalocyanine conjugate combining MRI contrast imaging and photosensitization properties as a potential molecular theranostic. Photochem Photobiol 90:1376–1386
16. Kupka T, Dzięgielewski JO, Pasterna G, Małecki JG (1992) Copper-D-penicillamine complex as potential contrast agent for MRI. Magn Reson Imaging 10:855–858
17. Moon HK, Son M, Park JE, Yoon SM, Lee SH, Choi HC (2012) Significant increase in the water dispersibility of zinc phthalocyanine nanowires and applications in cancer phototherapy. NPG Asia Mater 4:e12
18. Kliber M, Broda MA, Nackiewicz J (2016) Interactions of zinc octacarboxyphthalocyanine with selected amino acids and with albumin. Spectrochim Acta Part A 155:54–60
19. Fosmire GJ (1990) Zinc toxicity. Am J Clin Nutr 51:225–227

20. Scheidt WR, Dow W (1977) Molecular stereochemistry of phthalocyanatozinc(II). J Am Chem Soc 99:1101–1104
21. Mihill A, Buell W, Fink M (1993) Structure of zinc phthalocyanine by gas phase electron diffraction. J Chem Phys 99(9):6416–6420. https://doi.org/10.1063/1.465880
22. Ruan C-y, Mastryukov V, Fink M (1999) Electron diffraction studies of metal phthalocyanines, MPc, where M=Sn, Mg, and Zn (re-investigation). J Chem Phys 111(7):3035–3041. https://doi.org/10.1063/1.479584
23. Templeton DH, Fischer MS, Zalkin A, Calvin M (1971) Structure and chemistry of the porphyrins. Crystal and molecular structure of the monohydrated dipyridinated magnesium phthalocyanine complex. J Am Chem Soc 93:2622–2628
24. Kobayashi T, Ashida T, Uveda N, Suito E, Kakudo M (1971) The crystal structure of the 2 : 3 complex of zinc phthalocyanine and n-hexylamine. Bull Chem Soc Jpn 44:2095–2103
25. Schannon RD (1976) Revised effective ionic radii and systematic studies of interatomic distances in halides and chalcogenides. Acta Crystal A32:751–767
26. Przybył B, Janczak J (2014) Structural characterisation and DFT calculations of three new complexes of zinc phthalocyanine with n-alkylamines. Dyes Pigments 100:247–254
27. Plows FL, Jones AC (1999) Laser-desorption supersonic jet spectroscopy of phthalocyanines. J Mol Spectrosc 194:163–170
28. Ramachandran KI, Deepa G, Namboori K (2008) Computational chemistry and molecular modeling principles and applications. Springer-Verlag GmbH, Berlin-Heidelberg
29. Jensen F (2007) Introduction to computational chemistry. John Wiley and Sons, Chichester
30. Hohenberg P, Kohn W (1964) Inhomogeneous electron gas. Phys Rev 136:B864–B871
31. Kohn W, Sham LJ (1965) Self-consistent equations including exchange and correlation effects. Phys Rev 140:A1133–A1138
32. Parr RG, Yang W (1989) Density theory of atoms and molecules. Oxford University Press, New York
33. Liao M-S, Scheiner S (2002) Comparative study of metal-porphyrins, porphyrazines, and -phthalocyanines. J Comput Chem 23: 1391–1403
34. Tackley DR, Dent G, Smith WE (2000) IR and Raman studies for zinc phthalocyanine from DFT calculations. Phys Chem Chem Phys 2:3949–3955
35. Strenalyuk T, Samdal S, Volden HV (2007) Molecular structures of phthalocyaninatozinc and hexadecafluorophthalocyaninatozinc studied by gas-phase electron diffraction and quantum chemical calculations. J Phys Chem A 111:12011–11218
36. Becke AD (1993) Density-functional thermochemistry. III. The role of exact exchange. J Chem Phys 98(7):5648–5652
37. Lee C, Yang W, Parr RG (1988) Development of the Colle-Salvetti correlation-energy formula into a functional of the electron density. Phys Rev B 37(2):785–789
38. Miehlich B, Savin A, Stoll H, Preuss H (1989) Results obtained with the correlation-energy density functionals of Becke and Lee, Yang and Parr. Chem Phys Lett 157:200–206
39. Liu X, L-C X, He TJ, Chen D-M, Liu F-C (2003) Density functional theory investigations of geometries and electronic spectra of lithium phthalocyanines. Chem Phys Lett 379:517–525
40. Miertus S, Scrocco E, Tomasi J (1981) Electrostatic interaction of a solute with a continuum. A direct utilization of ab initio molecular potentials for the prevision of solvent effects. Chem Phys 55:117–129
41. Ueno LT, Machado AEH, Machado FBC (2009) Theoretical studies of zinc phthalocyanine monomer, dimer and trrimer forms. J Mol Struct (THEOCHEM) 899:71–78
42. Kekulé FA (1865) Sur la constitution des substances aromatiques. Bull Soc Chim Paris 3:98–110
43. Mucsi Z, Viskolcz B, Csizmadia IG (2007) A quantitative scale for the degree of aromaticity and Antiaromaticity. J Phys Chem A 111: 1123–1132
44. Pv RS, Manoharan M, Jiao H, Stahl F (2001) The Acenes: is there a relationship between aromatic stabilization and reactivity. Org Lett 3:3643–3646
45. Krygowski TM, Szatylowicz H, Stasyuk OA, Dominikowska J, Palusiak M (2014) Aromaticity from the viewpoint of molecular geometry: application to planar systems. Chem Rev 114:6383–6422
46. Kruszewski J, Krygowski TM (1972) Definition of aromaticity basing on the harmonic oscillator model. Tetrahedron Lett 13: 3839–3842
47. von Rague Schleyer P, Jiao H (1996) What is aromaticity? Pure Appl Chem 68:209–218
48. Krygowski TM, Szatyłowicz H (2015) Aromaticity: what does it mean? ChemTexts:1–12
49. Chen Z, Wannere CS, Corminboeuf C, Puchta R, Von Rague Schleyer P (2005) Nucleous-independent chemical shifts (NICS) as an aromaticity criterion. Chem Rev 105:3842–3888
50. Cyrański MK, Stępień BT, Krygowski TM (2000) Global and local aromaticity of linear and angular polyacenes. Tetrahedron 56:9663–9667
51. Dobrowolski JC, Lipiński PFJ (2016) On splitting of the NICS(1) magnetic aromaticity index. RSC Adv 6:23900–23904
52. Krygowski TM, Cyrański MK (2001) Structural aspects of aromaticity. Chem Rev 101:1385–1420
53. Ostrowski S, Dobrowolski JC (2014) What does the HOMA index realy measure? RSC Adv 4:44158–44161
54. Dobrowolski JC, Ostrowski S (2015) On the HOMA index of some acyclic and conducting systems. RSC Adv 5:9467–9471
55. Krygowski TM (1993) Crystallographic studies of inter- and intramolecular interactions reflected in aromatic character of "pi"-electron systems. Int Chem Inf Comput Sci 33:70–78
56. Pople JA, Untch JA (1966) Induced paramagnetic ring currents. J Am Chem Soc 88:4811–4815
57. Junqueira GMA, Dos Santos HF (2014) Theoretical study of the solvent effect on the aromaticity of benzene: a NICS analysis. J Mol Model 20:2152–2158
58. Ozimiński WP, Krygowski TM, Noorizadeh S (2012) Aromaticity of pentafulvene's complexes with alkaline metal atoms. Struct Chem 23:931–938
59. Ozimiński WP, Krygowski TM, Fowler PW, Soncini A (2010) Aromatization of fulvene by complexation with lithium. Org Lett 12:4880–4883
60. Cyrański MK, Krygowski TM, Wisiorowski M, van Eikema Hommes NJR, Von Rague Schleyer P (1998) Global and local aromaticity in porphyrins: an analysis based on molecular geometries and nucleus-independent chemical shifts. Angew Chem Int Ed 37:177–180
61. Zhao V, Truhlar DG (2008). Theor Chem Accounts 120:215–241
62. Zhao Y, Truhlar DG (2008) Density Functionals with broad applicability in chemistry. Acc Chem Res 41:157–167
63. Ditchfield R, Hehre WJ, Pople JA (1971) Self-consistent molecular-orbital methods. IX. An extended Gaussian-type basis for molecular-orbital studies of organic molecules. J Chem Phys 54: 724–728
64. Davidson ER, Feller D (1986) Basis set selection for molecular calculations. Chem Rev 86:681–696
65. Hehre WJ, Radom L, Schleyer PR, Pople JA (1986) Ab initio molecular orbital theory. Wiley, New York
66. Frisch MJ, Trucks GW, Schlegel HB, Scuseria GE, Robb MA, Cheeseman JR, Scalmani G, Barone V, Mennucci B, Petersson GA, Nakatsuji H, Caricato M, Li X, Hratchian HP, Izmaylov AF, Bloino J, Zheng G, Sonnenberg JL, Hada M, Ehara M, Toyota K, Fukuda R, Hasegawa J, Ishida M, Nakajima T, Honda Y, Kitao O,

Nakai H, Vreven T, Montgomery, JA Jr, Peralta JE, Ogliaro F, Bearpark M, Heyd JJ, Brothers E, Kudin KN, Staroverov VN, Keith T, Kobayashi R, Normand J, Raghavachari K, Rendell A, Burant JC, Iyengar SS, Tomasi J, Cossi M, Rega N, Millam JM, Klene M, Knox JE, Cross JB, Bakken V, Adamo C, Jaramillo J, Gomperts R, Stratmann RE, Yazyev O, Austin AJ, Cammi R, Pomelli C, Ochterski JW, Martin RL, Morokuma K, Zakrzewski VG, Voth GA, Salvador P, Dannenberg JJ, Dapprich S, Daniels AD, Farkas O, Foresman JB, Ortiz JV, Cioslowski J, Fox DJ (2013) Gaussian 09, Revision E.01. Gaussian, Inc., Wallingford CT

67. Foresman JB, Frisch A (1996) Exploring chemistry with electronic structure methods. Ed. Second edn, Gaussian Inc, Pittsburg, PA
68. Nazarski RB, Wałejko P, Witkowski S (2016) Multi-conformer molecules in solutions: an NMR-based DFT/MP2 conformational study of two glucopyranosides of a vitamin E model compound. Org Biomol Chem 11(3142–3158)
69. Radula-Janik K, Kupka T, Ejsmont K, Daszkiewicz Z, Sauer SPA (2016) DFT and experimental studies on structure and spectroscopic parameters of 3,6-diiodo-9-ethyl-9H-carbazole. Struct Chem 27: 199–207
70. Murray C, Dozova N, McCaffrey JG, FitzGerald S, Shafizadeh N, Crepin C (2010) Infra-red and Raman spectroscopy of free-base and zinc phthalocyanines isolated in matrices. Phys Chem Chem Phys 12:10406–10422
71. Semenov SG, Bedrina ME (2009) Highly symmetrical phthalocyanines and perfluorophthalocyanines: the quantum-chemical study. Rus J General Chem 79:1741–1747
72. Nguyen KA, Pachter R (2001) Ground state electronic structures and spectra of zinc phthalocyanine: a density functional theory study. J Chem Phys 114:10757–10767
73. Kupka T, Gerothanassis IP, Demetropoulos I (2000) Density functional study of a model amide. Prediction of formamide geometry, dipole moment, IR harmonic vibration ß c=o and GIAO NMR shieldings. J Mol Struct (THEOCHEM) 531:143–157
74. Cui L-Y, Yang J, Fu Q, Zhao B-Z, Tian L, H-L Y (2007) Synthesis, crystal structure and characterization of a new zinc phthalocyanine complex. J Mol Struct 827:149–154
75. Fischer MS, Templeton DH, Zalkin A, Calvin M (1971) Structure and chemistry of the porphyrins. The crystal and molecular structure of the monohydrated dipyridinated magnesium phthalocyanin complex. J Am Chem Soc 93:2622–2628
76. Yang Y (2010) Hexacoordinate bonding and aromaticity in silicon phthalocyanine. J Phys Chem A 114:13257–13267
77. Cissell JA, Vaid TP, DiPasquale AG, Rheingold AL (2007) Germanium phthalocyanine, GePc, and the reduced complexes SiPc(pyridine)2 and GePc(pyridine)2 containing antiaromatic π-electron circuits. Inorg Chem 46:7713–7715